Dual-Specificity Phosphatases Are Implicated in Severe Hyperplasia and Lack of Response to FGF23 of Uremic Parathyroid Glands from Rats

Pablo Román-García, Natalia Carrillo-López, Manuel Naves-Díaz, Isabel Rodríguez, Alberto Ortiz, and Jorge B. Cannata-Andía

Servicio de Metabolismo Óseo y Mineral (P.R.-G., N.C.-L., M.N.-D., I.R., J.B.C.-A.), Hospital Universitario Central de Asturias, Instituto Reina Sofía de Investigaciones Nefrológicas (IRSIN) and Universidad de Oviedo, 33006 Oviedo, Asturias, Spain; Red de Investigación Renal (RedInRen) (P.R.-G., N.C.-L., M.N.-D., I.R., A.O., J.B.C.-A.); and Servicio de Nefrología (A.O.), Instituto de Investigación Sanitaria (IIS) Fundación Jiménez Díaz, IRSIN and Universidad Autónoma de Madrid, 28049 Madrid, Spain

Phosphate load accelerates the progression of secondary hyperparathyroidism (sHPT). In advanced stages of sHPT, there is a marked hyperplasia and resistance to classical regulatory endocrine factors such as calcium, calcitriol, or fibroblast growth factor 23 (FGF23), which suppresses PTH secretion by an ERK-dependent mechanism. Nephrectomized rats were fed with a high- or normal-phosphorus diet for different periods of time to induce sHPT. Biochemical parameters, parathyroid gland microarrays, quantitative real-time PCR, and immunohistochemistry (ERK/phospho-ERK) were performed. To test the role of dual-specificity phosphatases (Dusp) on parathyroid gland regulation, normal parathyroid glands were cultured with FGF23 and Dusp. Uremic rats fed with a high-phosphorus diet showed more severe sHPT, higher serum FGF23 levels and mortality, and decreased parathyroid Klotho gene expression. In all stages of sHPT, parathyroid microarrays displayed a widespread gene expression down-regulation; only a few genes were overexpressed, among them, Dusp5 and -6. In very severe sHPT, a significant reduction in phospho-ERK (the target of Dusp) and a significant increase of Dusp5 and -6 gene expression were observed. In *ex vivo* experiments with parathyroid glands, Dusp partially blocked the effect of FGF23 on PTH secretion, suggesting that Dusp might play a role in parathyroid regulation. The overexpression of Dusp and the inactivation of ERK found in the *in vivo* studies together with the *ex vivo* results might be indicative of the defense mechanism triggered to counteract hyperplasia, a mechanism that can also contribute to the resistance to the effect of FGF23 on parathyroid gland observed in advanced forms of chronic kidney disease. **(*Endocrinology* 153: 1627–1637, 2012)**

Hyperplasia of the parathyroid glands is a common finding in patients with chronic kidney disease (CKD) and contributes to dysregulate the mineral balance. Excess of dietary phosphate accelerates the progression of secondary hyperparathyroidism (sHPT) (1) and increases vascular calcification as well (2, 3). In mild and early stages of CKD, parathyroid hyperplasia is at least partly reversible (4–6); in advanced and late stages, the enlarged parathyroid glands do not respond adequately to increments in serum calcium, high doses of active vitamin D, or high levels of fibroblast growth factor 23 (FGF23) due to several abnormalities in nucleic acid stability and repair (7). The uremic parathyroid glands also show decreased expression of the calcium-sensing receptor (CaSR), the vitamin D receptor (VDR), Klotho, and the FGF receptor 1, leading to a parathyroid resistance to their current endocrine regulatory factors (8–10).

In addition to the well-known role of calcium and calcitriol in the kidney-bone-parathyroid axis, it has been demonstrated that FGF23 suppresses PTH secretion by

ISSN Print 0013-7227 ISSN Online 1945-7170
Printed in U.S.A.

doi: 10.1210/en.2011-1770 Received September 16, 2011. Accepted January 12, 2012.
First Published Online February 14, 2012

Abbreviations: CaSR, Calcium-sensing receptor; CKD, chronic kidney disease; Dusp, dual-specificity phosphatase; FGF23, fibroblast growth factor 23; HPD, high-phosphorus diet; NPD, normal-phosphorus diet; OMFP, 3-*O*-methyl fluorescein phosphate; pERK, phospho-ERK; RT-qPCR, reverse transcription quantitative PCR; sHPT, secondary hyperparathyroidism; VDR, vitamin D receptor.

activating the ERK/MAPK pathway in the parathyroid glands (9). However, in sHPT, the inhibitory effect of FGF23 on PTH synthesis is not observed (9, 11). The absence of FGF23 inhibition of PTH synthesis has been recently associated with the low levels of Klotho/FGF receptor 1 found in parathyroid glands from uremic patients or animals (10, 12).

The present experimental study was designed to assess parathyroid hyperplasia secondary to CKD, by analyzing the gene expression profile changes across different stages of hyperparathyroidism. In addition, we also aimed to elucidate functionally whether regulators of MAPK signaling might play a role in the FGF23 signaling in the parathyroid glands.

Materials and Methods

Animal model

The study was performed in 4-month-old male Wistar rats. The initial number of rats, including the rats that did not finish the study, was 111. Rats were anesthetized using methoxyflurane, and chronic renal failure was induced by surgical seven eighths nephrectomy (13). The nephrectomized rats were subsequently divided into two groups: group 1 was fed with an normal-phosphorus diet (NPD: 0.6% phosphorus, 0.6% calcium, and 20% protein content), and group 2 was fed with a high-phosphorus diet (HPD: 0.9% phosphorus, 0.6% calcium, and 20% protein content) (Panlab, Barcelona, Spain). Rats were housed in wire cages and received diet and water *ad libitum*.

Five rats from the HPD and NPD groups were killed by heart-puncture exsanguination after 4, 8, 12, 16, and 20 wk of follow-up. When the rats were killed, blood samples and parathyroid glands were obtained (14). An additional group of rats without nephrectomy was fed with an NPD for 20 wk and used as the reference group (n = 9). The total number of groups studied was 11.

Because the aim of the present study was to investigate parathyroid gland regulation across different stages of hyperparathyroidism, we decided to use PTH values and HPD exposure as the main parameters to form the three groups of study: moderate sHPT, which included rats from the all NPD subgroups showing serum PTH values below 150 pg/ml; moderate-severe sHPT, which included rats from the HPD subgroups from wk 4, 8, and 12 showing values between 151 and 1000 pg/ml; and very severe sHPT, which included rats from the HPD subgroups from wk 16 and 20 showing values above 1001 pg/ml. Thus, 59 rats were used and distributed as follows: moderate sHPT, 25 rats; moderate/severe sHPT, 15 rats; very severe sHPT, 10 rats; and reference group, nine rats. This strategy was also used to analyze and compare the rest of the parameters.

The Laboratory Animal Ethics Committee of the Universidad de Oviedo approved this protocol.

Biochemical markers

Serum was separated from blood samples by centrifugation at 4000 rpm at 4 C. Serum urea, creatinine, calcium, and phosphorus were measured using a multichannel Auto Analyzer (Hitachi 717, Boehringer Mannheim, Berlin, Germany) following the manufacturer's protocol. Serum PTH was measured using an immunoradiometric rat PTH assay with a specific chicken anti-PTH antibody, following the manufacturer's protocol (Immutopics, San Juan Capistrano, CA) (normal range, 10–30 pg/dl). Serum FGF23 was measured using an ELISA following the manufacturer's protocol (60-6300; Immutopics) (normal ranges, 800-1000 pg/ml).

Gene expression microarrays

The parathyroid glands (one per rat) from each subgroup were pooled and homogenized (Ultraturrax, OmniHT, Kennesaw, GA) in TRI reagent (Sigma-Aldrich, St. Louis, MO). Total RNA was extracted and purified using an RNeasy Kit (QIAGEN Inc., Valencia, CA). RNA integrity was checked using agarose-formaldehyde gels, and RNA concentration was measured using a VIS-UV spectrophotometer (Nanodrop Tech., Wilmington, DE). cDNA was synthesized with a High Capacity kit (Applied Biosystems, Foster City, CA), and hybridized to one Affy RAE_230 cDNA microarray (Affymetrix, Santa Clara, CA) following the required quality controls and the manufacturer's protocol. The array included all rat genes (31,099 probes per array). As a result of the pooling, we obtained one array per each of the 11 subgroups, and we formed the groups following the criteria explained above.

To analyze the raw datasets, data were logarithmically transformed and normalized using the PerfectMatch/MisMatch method (dChip) (15), with the reference group as baseline comparator. After the normalization and expression modeling of the raw data, we followed a two-step process. In the first step, to investigate specific differences among the samples in selected genes, hierarchical clusters were built using the Euclidean-Centroid Linkage method. Two types of clusters were built: 1) unsupervised clusters, in which all genes were included to investigate general differences in the pattern of expression among the samples, and 2) supervised clusters, in which specific genes grouped by ontology terms (obtained from the Kyoto Encyclopedia of Genes and Genomes) were included. In the second step, different comparisons were performed (moderate *vs.* very severe sHPT, moderate *vs.* moderate-severe sHPT, and moderate-severe *vs.* very severe sHPT) using ANOVA and Student's *t* tests depending on the comparisons. Afterward, a fold change was adjudicated using a false discovery rate algorithm to avoid false positives. Only the probes with fold changes more than +2 or less than −2 were selected.

Reverse Transcription Quantitative PCR (RT-qPCR)

Genes of interest selected from the microarrays were validated by RT-qPCR (ABI Prism 7000, Applied Biosystems), using TaqMan predeveloped assays: *Dusp6* (Rn_00518185_m1) and *Dusp5* (Rn_0683448_m1). In addition, other genes related to sHPT such as *Pth* (Rn00566882_m1), *Casr* (Rn 00566496_m1), *Klotho* (Rn00580132_m1), and *Vdr* (Rn00566976_m1) were analyzed. As endogenous control, *18s* (eukaryotic 18s rRNA endogenous control reagent; Applied Biosystems) and *Gapdh* (Rn99999916_m1) were used.

Immunohistochemistry

The presence of ERK and phospho-ERK (pERK) in parathyroid tissue was also determined by immunohistochemistry in 5-μm-thick serial sections from paraffin-embedded parathyroid glands using specific antibodies (Cell Signaling Technology Inc., Danvers, MA; item nos. 9106 and 9102, respectively) and hematoxylin counterstaining (HistoStainPlus IHC detection Kit; Invitrogen for Life Technologies Corporation, Carlsbad, CA) following the manufacturer's instructions. A negative control without primary antibody was used. For the quantification of the staining, a Leica CTR-Mic microscope coupled to image analysis software (Leica Q500IW, Leica, Weztlar, Germany) was used. Briefly, the image of each gland was converted to grayscale. Then, using the OD function of the software, pixels that fell within a designed threshold were used and counted; as a result, we obtained a mean of gray color. Brown *et al.* (16) described the complete method.

Parathyroid *ex vivo* tissue culture

Parathyroid glands were obtained from 3-month-old male Wistar rats (n = 96), with normal renal function, as described (14). The Laboratory Animal Ethics Committee of the Universidad de Oviedo approved this protocol.

The glands were washed for 8 h in standard medium (17) containing 1.2 mM Ca. After the washing period, the glands were treated for an additional 24 h with the standard medium or with a medium containing 0.6 mM calcium, alone or in combination with different factors. This very same approach has been published in previous studies related to PTH synthesis and secretion (17). As a result, five groups were obtained: 1) 1.2 mM Ca, 2) 0.6 mM Ca, 3) 0.6 mM Ca plus FGF23 100 ng/ml (2629-FG; R&D Systems Inc., Minneapolis, MN), 4) 0.6 mM Ca plus FGF23 100 ng/ml plus UO126 1 μM (UO126, U-120; Sigma Aldrich), and 5) 0.6 mM Ca plus FGF23 100 ng/ml plus a mixture of recombinant dual-specificity phosphatase (Dusp) at 1 μl/ml each (AK-020; BIOMOL International for Enzo Life Sciences Inc., Farmingdale, NY). The activity of the Dusp ranged between an interval of 5–90 U/μg depending on the specific Dusp. It was assayed by 3-*O*-methyl fluorescein phosphate (OMFP) hydrolysis at 30 C. The assay conditions were 1 μg enzyme per 100 μl in 100 mM Tris-HCl (pH 8.2), 40 mM NaCl, 1 mM dithiothreitol, 20% glycerol, and 0.5 mM OMFP. One unit was equal to 1 pmol phosphate

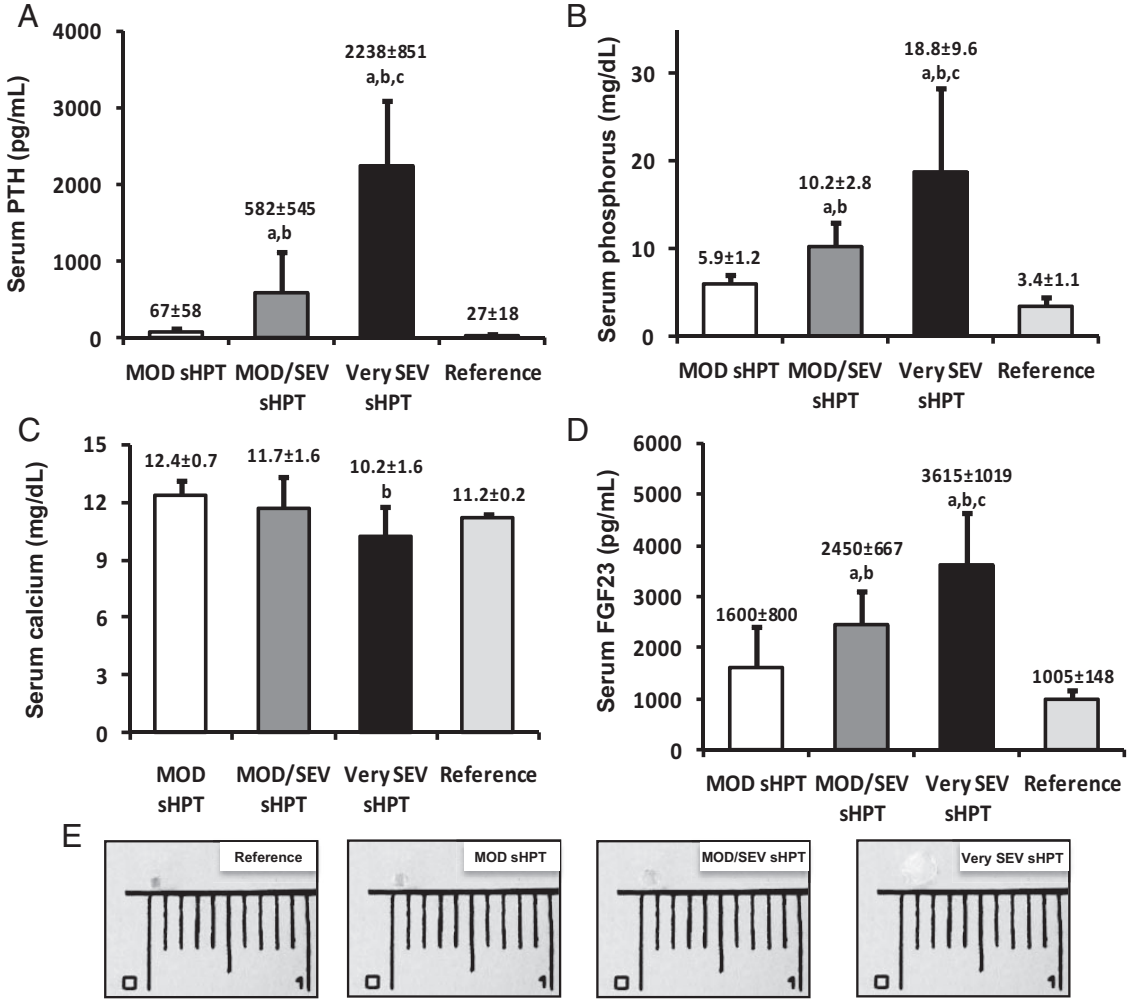

FIG. 1. A–D, Mean ± SD of serum levels of PTH (A), phosphorus (B) , calcium, (C), and FGF23 (D) from the reference, moderate (MOD sHPT), moderate-severe (MOD/SEV sHPT), and very severe sHPT (Very SEV sHPT) groups; E, representative image of one parathyroid gland from each group. ANOVA *P* value was <0.05 for all the parameters. The number of rats used was 25, 15, 10, and nine for very severe, moderate/severe, moderate sHPT, and reference groups, respectively. a, $P < 0.01$ compared with reference group; b, $P < 0.05$ compared with moderate sHPT group; c, $P < 0.05$ compared with moderate sHPT group (Tukey's *post hoc* analysis).

hydrolyzed from OMFP per minute. Six independent experiments were performed in each group. At the end, 192 parathyroid glands were used and distributed as follows: 1.2 mM Ca group, 32 parathyroid glands (16 rats); 0.6 mM Ca group, 40 parathyroid glands (20 rats); 0.6 mM Ca plus FGF23 group, 40 parathyroid glands (20 rats); 0.6 mM Ca plus FGF23 plus UO126 group, 40 parathyroid glands (20 rats); and 0.6 mM Ca plus FGF23 plus recombinant Dusp group, 40 parathyroid glands (20 rats).

PTH secretion was measured in the culture media at the beginning and at the end of all experiments using an ELISA following the manufacturer's protocol (60-2500; Immutopics).

Statistical analysis

One-way ANOVA with Tukey *post hoc* analyses were used to compare biochemical parameters among the groups as well as immunohistochemistry quantification, gene expression, and the *ex vivo* experiment's PTH secretion data. Data are expressed as mean ± SD. Differences were considered significant when $P < 0.05$. Calculations were performed using the statistical analysis package SPSS version 12.0 (SPSS Inc., Chicago, IL), dChip, R software and PASW version 17.0 (IBM, Corporation, Armonk, NY).

Results

Effects of HPD in uremic rats

Different degrees of sHPT were induced in uremic rats by feeding with a HPD or NPD for different time periods. In general terms, a longer exposure to HPD led to a more severe sHPT.

A total of 111 rats were included in the study and we observed different percentages of mortality according to degree of sHPT reaching 50, 40, and 25% in the very severe, moderate-severe, and moderate sHPT groups, respectively. Only rats that survived were analyzed.

Serum PTH, phosphorus, and FGF23 levels were significantly higher in the moderate-severe and very severe sHPT groups compared with the other two groups (Fig. 1, A, B, and D). In addition, significantly lower serum calcium levels were observed in the moderate-severe and very severe sHPT groups (Fig. 1C).

Serum FGF23 levels correlated positively with serum PTH (r = 0.83; $P < 0.01$; Fig. 2A) and with serum phosphorus (r = 0.76; $P < 0.05$; Fig. 2B).

The decrease in renal function was more marked in the very severe sHPT group, which showed significantly higher levels of serum urea and creatinine compared with the moderate and moderate-severe sHPT groups (data not shown). In fact, serum creatinine (r = 0.88; $P < 0.001$; Fig. 2C) and urea (r = 0.77; $P < 0.001$; Fig. 2D) levels positively correlated with serum PTH levels.

Gene expression analyses

In the first step, unsupervised hierarchical clusters (HC) from the microarray data [including all probes (31,099)

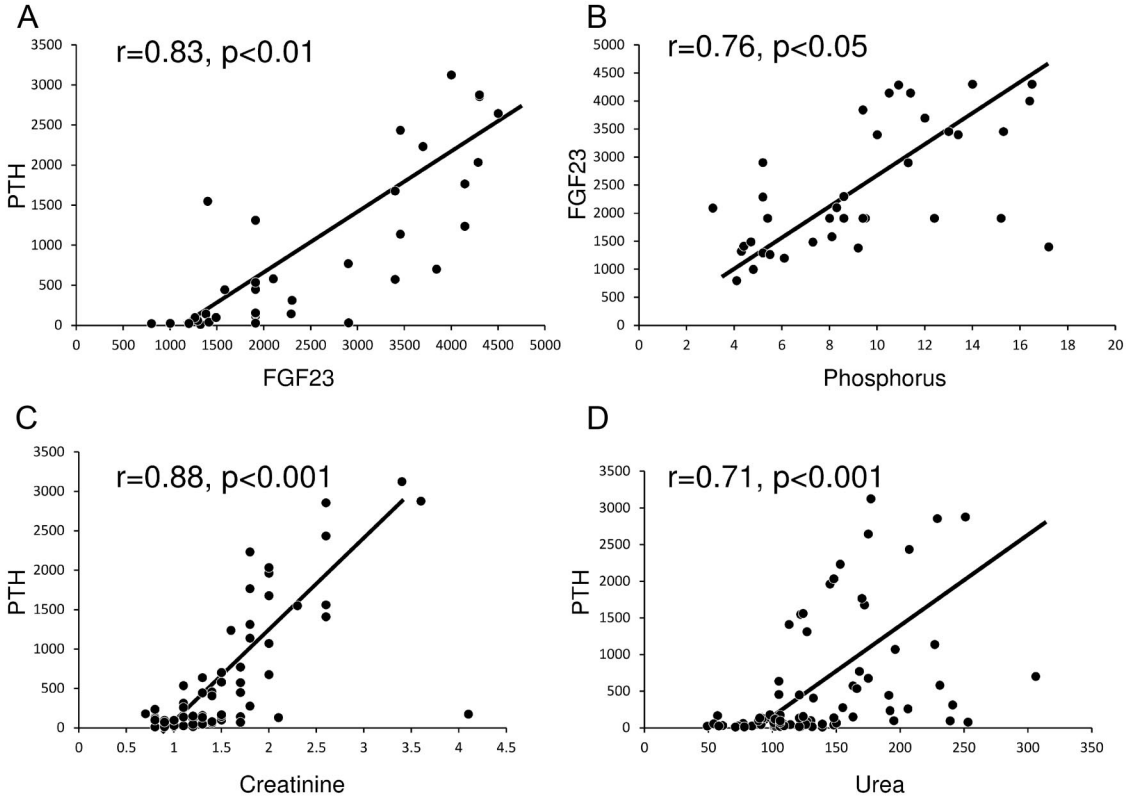

FIG. 2. Graphical representation of the Pearson correlations between serum PTH and FGF23 (A), serum FGF23 and phosphorus (B), serum PTH and creatinine (C), and serum PTH and urea (D). Units are milligrams per deciliter for creatinine and urea and picograms per milliliter for PTH and FGF23. The number of rats used was 59.

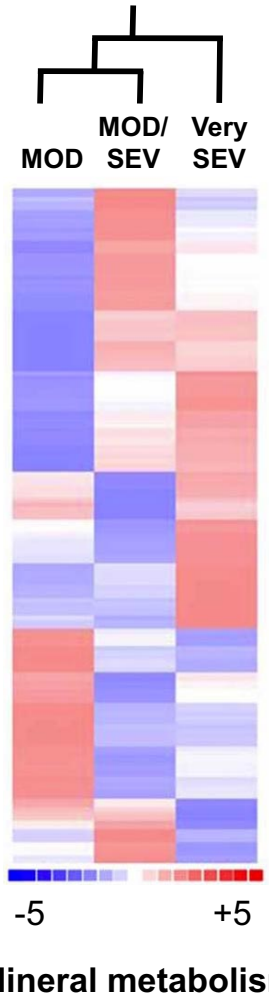

FIG. 3. Hierarchical clusters obtained from the microarray data of all groups using only those genes related to mineral metabolism. MOD, Moderate sHPT; MOD/SEV, moderate-severe sHPT; Very SEV, very severe sHPT.

and the different groups] showed that the very severe sHPT group was the only one segregated from the others (data not shown). By contrast, in the case of mineral metabolism-associated genes, the very severe sHPT group showed a remarkably different pattern of expression and clustered separately from the moderate and moderate-severe sHPT groups (Fig. 3).

In the second step, using the criteria explained in *Materials and Methods*, 136 probes were found to be differentially expressed in the very severe *vs.* moderate sHPT comparison (Table 1), 32 in the moderate-severe *vs.* moderate sHPT comparison, and 10 in the very severe *vs.* moderate-severe sHPT comparison (Supplemental Tables 1 and 2, published on The Endocrine Society's Journals Online web site at http://endo.endojournals.org).

Overall, a widespread down-regulation of gene expression was observed, involving more than 80% of the genes. Only a minor percentage of genes were up-regulated. Among the latter, the Dusp6 gene showed the highest overexpression in all the comparisons. Dusp5 was also up-regulated in the very severe *vs.* moderate sHPT comparison.

RT-qPCR experiments confirmed a very high up-regulation of Dusp6 gene expression in very severe sHPT (mean, 43-fold increase relative to the reference group) and also in moderate-severe sHPT (mean, 3.27-fold increase). Dusp5 gene expression also showed a significant 7.09-fold up-regulation in very severe sHPT but not in the moderate and moderate-severe sHPT subgroups.

Microarray analysis did not disclose significant differences in the gene expression of classical parathyroid regulators such as CaSR, VDR, or PTH. This is not a surprising result given that microarray analysis is a screening technology and the strict criteria applied to prevent false positives may have increased the number of false-negative findings or the number of genes below the threshold, including the aforementioned classical genes. In RT-qPCR analyses of the same parathyroid samples, CaSR, VDR, and Klotho gene expression were also significantly reduced in the very severe sHPT group, whereas PTH was progressively up-regulated (Fig. 4). The difference in Klotho expression between moderate and moderate-severe groups was not statistically significant, and it was under the limit of detection of the qRT-PCR (1.89-fold increase).

Activation of ERK in parathyroid glands

Dusp are protein phosphatases that dephosphorylate a specific MAPK, inhibiting its function. In particular, Dusp5 and Dusp6 specifically dephosphorylate and inactivate pERK1 and -2 (pERK1/2). Therefore, we analyzed the activation of ERK by immunohistochemistry analysis of ERK and pERK1/2 in paraffin-embedded parathyroid tissue. ERK staining was similar in all sHPT groups and the reference group. However, the intensity of pERK staining increased significantly in moderate sHPT when compared with the reference group. Interestingly, pERK decreased as the severity of sHPT increased, and it was significantly reduced in the very severe sHPT group compared with the moderate sHPT group (Fig. 5, A and B).

Evaluation of the role of Dusp on PTH secretion

To test whether Dusp might have a regulatory effect on parathyroid function, additional experiments were performed using parathyroid glands from normal rats cultured *ex vivo*. After 24 h in a medium containing 0.6 mM calcium showed the expected significant increase in PTH

TABLE 1. Gene expression dataset of the differentially expressed probes sorted by fold change, corresponding to the comparison of severe *vs.* moderate sHPT groups

Probe set	Gene	Accession	Fold change	*P* value
1372208_at	Protein phosphatase 1, regulatory (inhibitor) subunit 1B	AA942959	−15.51	0.002337
1370124_at	Metallothionein 3	NM_053968	−14.73	0.000024
1378692_at	Paired box gene 8	BF564165	−12.4	0.001508
1373631_at	RAP1, GTPase-activating protein 1	BF284067	−12.29	0.007627
1374070_at	Glutathione peroxidase 2	AA800587	−11.61	0.026228
1379390_at	ST6 (α-*N*-acetyl-neuraminyl-2,3-β-galactosyl-1,3)-*N*-a	AA891414	−10.29	0.011152
1367904_at	Regulated endocrine-specific protein 18	NM_019278	−9.95	0.023551
1371048_at	Forkhead box E1 (thyroid transcription factor 2)	Y11321	−9.86	0.011032
1391194_at	Sal-like 1 (*Drosophila*) (predicted)	BG377337	−9.83	0.012785
1370764_a_a	Thyroglobulin	M35965	−9.78	0.001381
1373915_at	Dystrophia myotonica-protein kinase (predicted)	AI044427	−9.4	0.00063
1370775_a_a	Calcitonin/calcitonin-related polypeptide, α	MI11597	−9.16	0.020795
1393335_at	EGF-like-domain, multiple 6	BF418373	−8.98	0.000275
1370973_at	Sodium channel, voltage-gated. type VII α	BF285019	−8.87	0.000088
1369784_at	Thyroid peroxidase	NM_019353	−8.78	0.001976
1389470_at	Complement factor B	AI639117	−8.72	0.002546
1371010_at	Thyroid transcription factor 1	BF389361	−8.31	0.000371
1370384_a_a	Prolactin receptor	M57668	−8.14	0.000106
1377353_a_a	TNF (ligand) superfamily, member 13	AA800814	−8.01	0.018282
1374775_at	Antigen identified by monoclonal antibody Ki-67 (predicted)	AI714002	2.15	0.03131
1369156_at	Fyn-related kinase	NM_024368	2.28	0.023371
1373658_at	Rac GTPase-activating protein 1 (predicted)	AI409259	2.3	0.008934
1383447_at	Ets variant gene S (ets-related molecule) (predicted)	AI101323	2.35	0.031435
1371875_at	Mannosidase, βA, lysosomal	BM388852	2.46	0.007069
1380775_at	M-phase phosphoprotein 1 (predicted)	BE110723	2.46	0.011388
1382122_at	Ets variant gene 5 (ets-related molecule) (predicted)	BE113124	2.6	0.008857
1370391_at	Cellular retinoic acid-binding protein 2	U23407	2.71	0.012111
1388253_at	Stearoyl-coenzyme A desaturase 2	M15114	2.79	0.022646
1389403_at	Bone morphogenetic protein 7	AI013715	2.83	0.002196
1367776_at	Cell division cycle 2 homolog A (*S. pombe*)	NM_019296	2.86	0.039293
1389566_at	Cyclin B2	AW253821	2.86	0.007195
1388484_at	Ubiquitin-conjugating enzyme E2C (predicted)	BI296084	2.99	0.009501
1369436_at	Cholinergic receptor, nicotinic, α polypeptide 10	NM_022639	3.01	0.044713
1370449_at	Purinergic receptor P2Y, G protein-coupled, 14	U76206	3.12	0.009019
1390918_at	GH-regulated TBC protein 1	BE099056	3.19	0.015337
1369972_at	Serine (or cysteine) peptidase inhibitor, clade B, member 5	NM_057108	3.27	0.033223
1378658_at	Chloride channel calcium activated 6	BI292185	3.39	0.00023
1377006_at	Chaperonin subunit 6a (ζ)	AA875047	3.47	0.001908
1375788_at	Ribosomal protein L7	BM388719	3.52	0.000331
1368266_at	Arginase 1	NM_017134	3.55	0.000472
1368124_at	Dusp5	NM_133578	3.57	0.034395
1381533_at	ρ-Family GTPase 1	AI144754	3.68	0.03904
1382803_at	MAPK kinase kinase kinase 1 (predicted	AI237423	3.78	0.003315
1390797_at	Lymphocyte cytosolic protein 2	BF282471	3.82	0.026496
1370090_at	Lymphocyte cytosolic protein 2	NM_130421	3.89	0.003265
1369525_at	GATA binding protein 3	NM_133293	3.98	0.000253
1389408_at	Ribonucleotide reductase M2 (mapped)	BG379338	3.98	0.041589
1390358_at	Calcium channel, voltage-dependent, α2/δ3 subunit	BF405996	6.3	0.028359
1370064_at	Presenilin 2	AB004454	8.25	0.03509
1387024_at	Dusp6	NM_053883	9.74	0.032946
1382778_at	Dusp6	AI231350	9.92	0.014481
1377064_at	Dusp6	AI602811	11.72	0.031855

Due to the elevated number of down-regulated genes (101), this table shows only the down-regulated probes that had a fold change lower than −8.

secretion compared with the glands cultured in a standard medium (1.2 mM calcium). By contrast, when glands were cultured in a medium containing 0.6 mM calcium plus 100 ng/ml FGF23, PTH secretion decreased significantly, down to the levels observed when using the standard medium. The effect of FGF23 on PTH secretion was ablated by the addition of a chemical ERK1/2 inhibitor (UO126, 1 μM), and consequently, PTH secretion was restored completely. The effect of FGF23 in PTH secretion was also partially blocked by adding Dusp, which

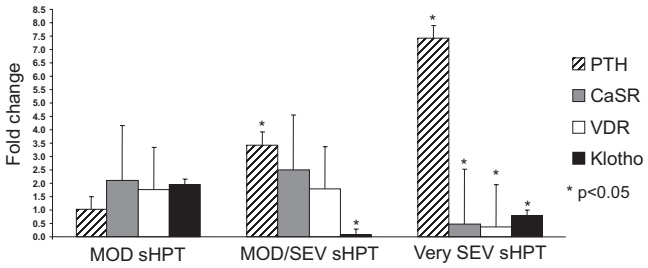

FIG. 4. Parathyroid gland PTH, CaSR, VDR, and Klotho mRNA levels measured by RT-qPCR in the moderate (MOD sHPT), moderate-severe (MOD/SEV sHPT), very severe sHPT (Very SEV sHPT), and reference group, which was given a reference value of 1. Data represent the mean of relative expression from the subgroups within the three groups. Mean ± SD values are shown. ANOVA *P* value was <0.05 for all the genes. *, $P < 0.05$ compared with moderate group when using Tukey's *post hoc* analysis.

are the biological inhibitors of the phosphorylation of ERK, resulting in a partial but significant restoration of PTH secretion (Fig. 6).

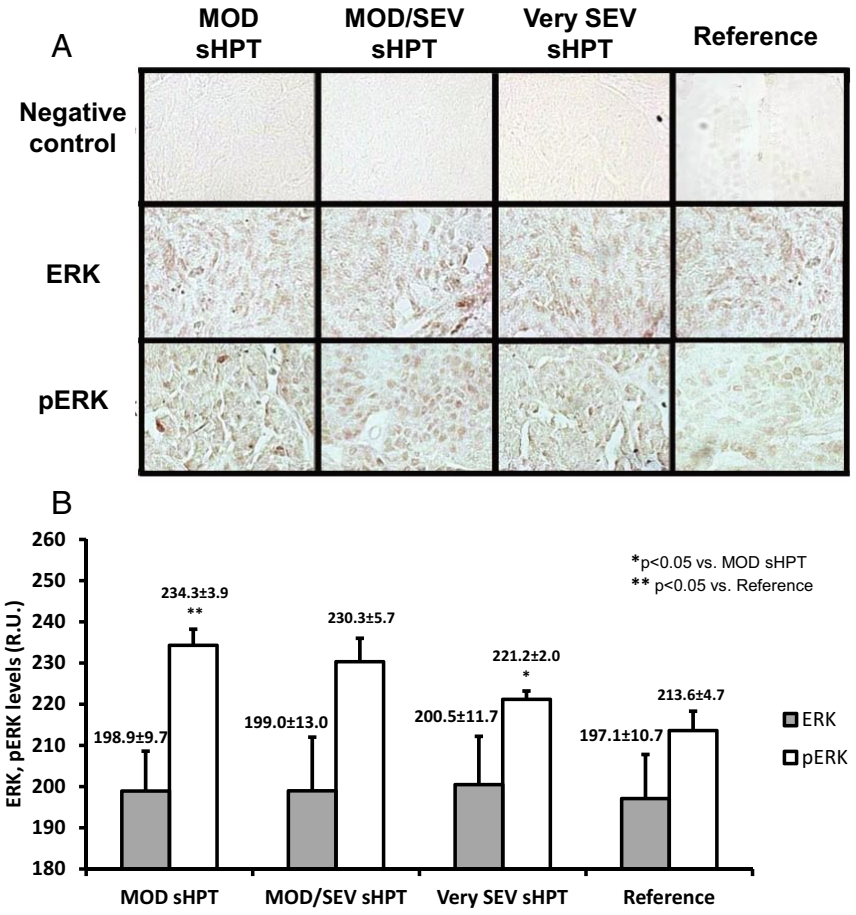

FIG. 5. Parathyroid gland total ERK1/2 and pERK1/2 protein staining. A, Representative images of immunohistochemistry from the reference, moderate sHPT (MOD), moderate-severe sHPT (MOD/SEV), and very severe sHPT (Very SEV) groups; B, quantification of the levels of total ERK and pERK in parathyroid glands. Reference group values for ERK and pERK are 197 ± 10.7 and 213 ± 4.69, respectively. Mean ± SD values are shown. ANOVA *P* value was <0.05. The number of rats used was 25, 15, 10, and nine for very severe, moderate/severe, moderate sHPT, and reference groups, respectively. *, $P < 0.05$ compared with moderate sHPT group; **, $P < 0.05$ compared with reference group (Tukey's *post hoc* analysis). R.U., Relative units.

Discussion

sHPT, vascular calcification, bone loss, and an increased fracture rate are severe and threatening alterations in general and also in the CKD population at all stages (18). Elevated serum phosphorus has been described as a major pathogenic player associated with sHPT progression but also to impairment of renal function, vascular calcification, and high risk of mortality; thus, phosphate load challenges the endocrine bone-kidney-parathyroid axis, contributing to the dysregulation of the mineral homeostasis (2, 19–21).

We observed that the degree of severity of sHPT was proportional to the time of exposure to a HPD (22, 23). In addition, we also observed that the HPD impaired renal function and increased mortality. As in other studies, we have also found a significant increase of FGF23 levels in all groups (compared with reference), which were higher in more severe sHPT; in fact, a direct correlation between serum FGF23 and PTH was found (24, 25). Both facts are frequently interpreted as a loss of the capability of FGF23 to inhibit PTH secretion, the resistance-to-FGF23 concept. Furthermore, serum FGF23 and phosphorus levels were also associated. The positive correlation of serum phosphorus with FGF23 and PTH, together with the higher values of these biochemical parameters observed in rats with the lowest renal function, may be indicative of a compensatory phosphaturic response via FGF23 and PTH, which was unable to fully compensate the decreased glomerular phosphate filtration.

To our knowledge, the gene expression microarray analysis shown in this study is the first carried out in parathyroid glands from rats. It clearly revealed that sHPT progression is characterized by a widespread gene expression down-regulation, as opposed to the gene expression up-regulation observed in primary hyperparathyroidism (7, 26). Because the very severe sHPT clustered separately from the moderate-severe and moderate sHPT groups (when the samples were clustered using mineral metabolism-associated genes), we can hypothesize that the more important changes in gene expression took place

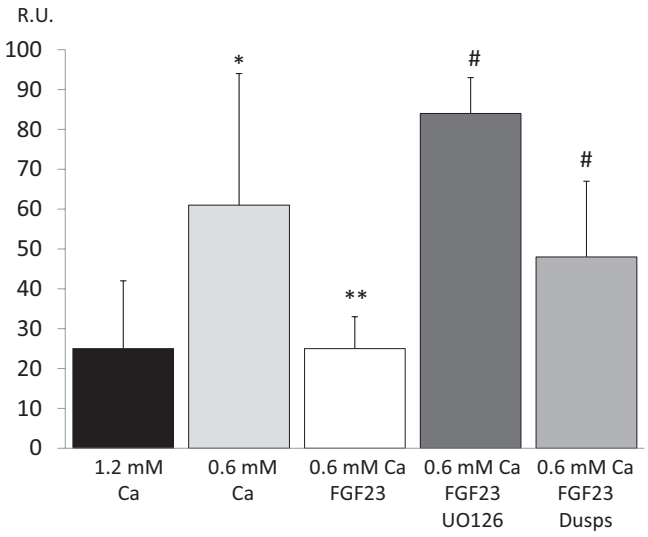

FIG. 6. PTH secretion in normal parathyroid glands cultured with 1.2 mM calcium, 0.6 mM Ca, 0.6 mM Ca plus FGF23, 0.6 mM Ca plus FGF23 plus UO126, and 0.6 mM Ca plus FGF23 plus Dusp. Six independent experiments were performed in triplicate. Number of glands in each group was as follows: 1.2 mM Ca group, 32 parathyroid glands (16 rats); 0.6 mM Ca group, 40 parathyroid glands (20 rats); 0.6 mM Ca plus FGF23 group, 40 parathyroid glands (20 rats); 0.6 mM Ca plus FGF23 plus UO126 group, 40 parathyroid glands (20 rats); and 0.6 mM Ca plus FGF23 plus Dusp group, 40 parathyroid glands (20 rats). Units are expressed as rate of change of PTH secretion ± SD. ANOVA P value was <0.05. *, $P < 0.05$ compared with 1.2 mM Ca group; **, $P < 0.005$ compared with 0.6 mM Ca group; #, $P < 0.02$ compared with 0.6 mM Ca plus FGF23 group (Tukey's *post hoc* analysis).

in advanced stages of sHPT. In addition, our molecular findings are consistent with previous data obtained in patients with severe nodular secondary and tertiary HPT (7) and also with current clinical responses, in whom mainly mild to moderate sHPT, but not the more severe forms of sHPT, are responsive to current therapies targeting the classical regulators.

In advanced sHPT, the abnormal control of PTH secretion has been partly attributed to CaSR and VDR down-regulation (8, 23). We did not find a significant deregulation of these genes using microarrays. It is known that microarray analysis has several limitations such as the underestimation or overestimation of gene expression (27). As described in *Results*, we used a very restrictive approach to avoid false positives, including the false discovery rate algorithm, and as a consequence, some of the classical genes known to be deregulated in CKD may have been automatically placed below the threshold. In addition, glands with severe degrees of sHPT show multiple genetic and molecular aberrations (7, 28), resulting in dramatic expression changes in some genes, which, after normalization, might mask or underestimate the changes in the classical genes. Validation by RT-qPCR, considered a valid method used as a supporting stepwise technique, is a widely accepted approach because it is far more sensitive and capable of detecting minor changes in specific genes. In fact, we did find significant up-regulation in PTH and down-regulation in CaSR, VDR, and Klotho gene expression in the very severe sHPT group when using RT-qPCR. These findings coincide with previous publications, which also have found a degree of down-regulation in the CaSR close to 50% or even less (16, 29, 30).

In our study, we found that the lack of the inhibitory effect of FGF23 on PTH secretion was associated with a down-regulation of Klotho gene expression. Similar findings were reported by three different previous studies (10, 12, 32), even though a recent paper described an up-regulation of Klotho in the parathyroid glands of uremic patients with severe sHPT (33). In addition, results from genetically modified mouse models suggest that FGF23 may be an indirect regulator of the parathyroid function (34). These controversial results are difficult to conciliate but could be partly explained by the difficulties associated with the quantification and interpretation of Klotho expression and the differences among the animal models used to investigate the role of FGF23 in mineral metabolism (11, 35).

Interestingly, in all comparisons (and irrespective of the groups compared), the repression of gene expression was the most common finding; only a very few genes were found to be overexpressed. Among them, Dusp6 was the one gene that always showed the highest degree of overexpression as confirmed by RT-qPCR. Dusp constitute a subclass of the protein phosphatase superfamily that dephosphorylates MAPK. Despite that MAPK signaling can be deactivated by changes in location or scaffolding, to our knowledge, the Dusp Family is the unique phosphatase system in charge of the dephosphorylation of MAPK (36). The members of the Dusp family exhibit high specificity against a single MAPK. A good example of their high specificity is the fact that Dusp6 and Dusp5 dephosphorylate and inactivate pERK1/2 but not other subclasses of MAPK such as c-Jun N-terminal kinase or p38 (37–39). The MAPK/ERK pathway is a very complex signaling mechanism that regulates mainly the cell cycle and proliferation (40). In the parathyroid gland, the MAPK/ERK pathway is activated with the development of sHPT (9, 41, 42) but is also part of the FGF23 intracellular signaling pathway that suppresses PTH secretion. In particular, ERK1/2 is required for FGF23-induced PTH suppression; in addition, ERK1/2 inhibitors prevent this suppression, and ERK inactivation has been recently described in FGF23-refractory parathyroid glands from uremic rats (9, 32). According to our results, a plausible explanation for the somewhat surprising dynamics of ERK is that in the initial stages of hyperparathyroidism, an increase of ERK

phosphorylation (a trigger to start hyperproliferation) can be observed. As hyperparathyroidism progresses to more severe forms, parathyroid cells would increase Dusp gene expression to reduce the high activity of the parathyroid gland through increased ERK phosphorylation as Dusp are expressed at low levels in nonstimulated cells and are induced as response genes in other stages (43).

As a result of this peak of transcription of Dusp, a significant decrease of pERK levels is observed only in the severe stages of parathyroid hyperplasia. Similar mechanisms have been previously described in lung cancer and myocardial cells (44, 45).

We hypothesize that the mechanisms to counteract excessive parathyroid growth, aiming to decrease MAPK pathway activation, are partly but not only driven by increases in Dusp in this advanced stage but to a lesser extent in previous stages, likely modifying FGF23 signal.

Interestingly, inactivation of ERK by the increased Dusp gene expression may contribute to the fact that FGF23 appears to have little suppressive effect on PTH secretion in severe forms of CKD. Indeed, several studies support that Dusp6 plays a key role as a specific negative-feedback regulator of FGF-activated ERK1/2 signaling (46).

To mechanistically confirm whether Dusp might play a role in FGF23 signaling, we performed additional experiments culturing normal parathyroid glands with FGF23 alone or in combination with UO126 (an ERK inhibitor) and recombinant Dusp. Following previous published results in which the functional capacity of fresh parathyroid glands maintained constant until 4 d (47), normal parathyroid glands were cultured with 0.6 mM calcium to secure PTH stimulation (17, 48). As expected, low calcium levels increased PTH secretion compared with standard calcium levels, which clearly suppress PTH. FGF23 reduced low calcium-induced PTH secretion in normal glands, to values similar to observed when using 1.2 mM calcium concentration, as previously described (9). The chemical ERK1/2 inhibitor (UO126) prevented the suppressive effect of FGF23 on PTH secretion, and interestingly, the addition of recombinant Dusp also prevented the FGF23 effect on PTH secretion. These findings strongly suggest that Dusp might regulate FGF23 signaling through MAPK inhibition. The fact that Dusp5 is a target of p53 (31) represents a feasible mechanism by which p53, activated in response to the observed DNA damage (26, 28) might negatively regulate cell-cycle progression by downregulating mitogen- or stress-activated protein kinases. The latter supports the hypothesis that Dusp could be implicated in the counterresponse to severe hyperplasia, likely via p53 activation, having an additional effect that would be the shutdown of FGF23 signaling in the parathyroid glands.

In summary, rats fed with a HPD showed a marked reduction in renal function, severe sHPT, high levels of FGF23, and a higher mortality. Despite that the parathyroid gene expression down-regulation was the predominant finding associated with sHPT, we observed a striking overexpression of Dusp and inactivation of the MAPK/ERK pathway. The latter might reflect a defensive mechanism triggered to counteract sHPT progression. In addition, the *ex vivo* results strongly suggest that increases in Dusp could contribute to the parathyroid FGF23 resistance. Altogether, our results allowed us to postulate that the overexpression of Dusp, with the associated inactivation of ERK, might play a regulatory role in parathyroid regulation in sHPT, partially blocking the intracellular FGF23 signaling pathway.

Acknowledgments

We thank Dr. Socorro Braga and Dr. Teresa Fernández-Coto for their assistance in the biochemical analyses, Dr. Daniel Álvarez-Hernández and Ángeles González-Carcedo for the valuable help with the animals, and Marino Santirso for the linguistic review of the text.

Address all correspondence and requests for reprints to: Jorge B. Cannata-Andía, Servicio de Metabolismo Óseo y Mineral, Instituto Reina Sofía de Investigación, Hospital Universitario Central de Asturias, C/ Julián Clavería s/n, 33006 Oviedo, Asturias, Spain. E-mail: metoseo@hca.es.

This work was supported by grants from the Fondo de Investigaciones Sanitarias (FIS 090415), Fundación para el Fomento en Asturias de la Investigación Científica Aplicada y Técnica (FICYT I30P06P), Instituto de Salud Carlos III (RETIC-RD06), Red de Investigación Renal (REDinREN 16/06), and Fundación Renal Íñigo Álvarez de Toledo.

Disclosure Summary: All authors have nothing to declare.

References

1. **Slatopolsky E** 1998 The role of calcium, phosphorus and vitamin D metabolism in the development of secondary hyperparathyroidism. Nephrol Dial Transplant 13(Suppl 3):3–8
2. **Román-García P, Carrillo-López N, Fernández-Martín JL, Naves-Díaz M, Ruiz-Torres MP, Cannata-Andía JB** 2010 High phosphorus diet induces vascular calcification, a related decrease in bone mass and changes in the aortic gene expression. Bone 46:121–128
3. **Giachelli CM** 2004 Vascular calcification mechanisms. J Am Soc Nephrol 15:2959–2964
4. **Slatopolsky E** 2003 New developments in hyperphosphatemia management. J Am Soc Nephrol 14:S297–S299
5. **Naveh-Many T, Rahamimov R, Livni N, Silver J** 1995 Parathyroid cell proliferation in normal and chronic renal failure rats. The effects of calcium, phosphate, and vitamin D. J Clin Invest 96:1786–1793

6. **Gutierrez O, Isakova T, Rhee E, Shah A, Holmes J, Collerone G, Jüppner H, Wolf M** 2005 Fibroblast growth factor-23 mitigates hyperphosphatemia but accentuates calcitriol deficiency in chronic kidney disease. J Am Soc Nephrol 16:2205–2215
7. **Santamaría I, Alvarez-Hernández D, Jofré R, Polo JR, Menárguez J, Cannata-Andía JB** 2005 Progression of secondary hyperparathyroidism involves deregulation of genes related to DNA and RNA stability. Kidney Int 67:2267–2279
8. **Rodriguez M, Canalejo A, Garfia B, Aguilera E, Almaden Y** 2002 Pathogenesis of refractory secondary hyperparathyroidism. Kidney Int Suppl 80:155–160
9. **Ben-Dov IZ, Galitzer H, Lavi-Moshayoff V, Goetz R, Kuro-o M, Mohammadi M, Sirkis R, Naveh-Many T, Silver J** 2007 The parathyroid is a target organ for FGF23 in rats. J Clin Invest 117:4003–4008
10. **Galitzer H, Ben-Dov IZ, Silver J, Naveh-Many T** 2010 Parathyroid cell resistance to fibroblast growth factor 23 in secondary hyperparathyroidism of chronic kidney disease. Kidney Int 77:211–218
11. **Lafage-Proust MH** 2010 Does the downregulation of the FGF23 signaling pathway in hyperplastic parathyroid glands contribute to refractory secondary hyperparathyroidism in CKD patients? Kidney Int 77:390–392
12. **Komaba H, Goto S, Fujii H, Hamada Y, Kobayashi A, Shibuya K, Tominaga Y, Otsuki N, Nibu K, Nakagawa K, Tsugawa N, Okano T, Kitazawa R, Fukagawa M, Kita T** 2010 Depressed expression of Klotho and FGF receptor 1 in hyperplastic parathyroid glands from uremic patients. Kidney Int 77:232–238
13. **Naves-Díaz M, Carrillo-López N, Rodríguez-Rodríguez A, Braga S, Fernández-Coto T, Lopez-Novoa JM, López-Hernández F, Cannata-Andía JB** 2010 Differential effects of 17β-estradiol and raloxifene on bone and lipid metabolism in rats with chronic kidney disease and estrogen insufficiency. Menopause 17:766–771
14. **Alvarez-Hernandez D, Gonzalez-Suarez I, Naves M, Carrillo-Lopez N, Fdez-Coto T, Fernandez-Martin JL, Cannata-Andia JB** 2005 Long-term response of cultured rat parathyroid glands to calcium and calcitriol: the effect of cryopreservation. J Nephrol 18:141–147
15. **Li C, Wong WH** 2001 Model-based analysis of oligonucleotide arrays: expression index computation and outlier detection. Proc Natl Acad Sci USA 98:31–36
16. **Brown AJ, Ritter CS, Finch JL, Slatopolsky EA** 1999 Decreased calcium-sensing receptor expression in hyperplastic parathyroid glands of uremic rats: role of dietary phosphate. Kidney Int 55:1284–1292
17. **Carrillo-López N, Alvarez-Hernández D, González-Suárez I, Román-García P, Valdivielso JM, Fernández-Martín JL, Cannata-Andía JB** 2008 Simultaneous changes in the calcium-sensing receptor and the vitamin D receptor under the influence of calcium and calcitriol. Nephrol Dial Transplant 23:3479–3484
18. **London GM, Marchais SJ, Guérin AP, Boutouyrie P, Métivier F, de Vernejoul MC** 2008 Association of bone activity, calcium load, aortic stiffness, and calcifications in ESRD. J Am Soc Nephrol 19:1827–1835
19. **Mathew S, Tustison KS, Sugatani T, Chaudhary LR, Rifas L, Hruska KA** 2008 The Mechanism of Phosphorus as a Cardiovascular Risk Factor in CKD. J Am Soc Nephrol 19:1092–1105
20. **Cannata-Andía JB, Rodríguez-García M, Carrillo-López N, Naves-Díaz M, Díaz-López B** 2006 Vascular calcifications: pathogenesis, management, and impact on clinical outcomes. J Am Soc Nephrol 17:S267–S273
21. **Huttunen MM, Tillman I, Viljakainen HT, Tuukkanen J, Peng Z, Pekkinen M, Lamberg-Allardt CJ** 2007 High dietary phosphate intake reduces bone strength in the growing rat skeleton. J Bone Miner Res 22:83–92
22. **Almaden Y, Hernandez A, Torregrosa V, Canalejo A, Sabate L, Fernandez Cruz L, Campistol JM, Torres A, Rodriguez M** 1998 High phosphate level directly stimulates parathyroid hormone secretion and synthesis by human parathyroid tissue in vitro. J Am Soc Nephrol 9:1845–1852
23. **Silver J** 2000 Molecular mechanisms of secondary hyperparathyroidism. Nephrol Dial Transplant 15(Suppl 5):2–7
24. **Gutiérrez OM, Mannstadt M, Isakova T, Rauh-Hain JA, Tamez H, Shah A, Smith K, Lee H, Thadhani R, Jüppner H, Wolf M** 2008 Fibroblast growth factor 23 and mortality among patients undergoing hemodialysis. N Engl J Med 359:584–592
25. **Block GA, Klassen PS, Lazarus JM, Ofsthun N, Lowrie EG, Chertow GM** 2004 Mineral metabolism, mortality, and morbidity in maintenance hemodialysis. J Am Soc Nephrol 15:2208–2218
26. **Santamaria I, Alvarez-Hernandez D, Cannata-Andia JB** 2005 Genetics and molecular disorders in severe secondary hyperparathyroidism: lessons from RNA and microarray studies. J Nephrol 18:469–473
27. **Zhang M, Zhang L, Zou J, Yao C, Xiao H, Liu Q, Wang J, Wang D, Wang C, Guo Z** 2009 Evaluating reproducibility of differential expression discoveries in microarray studies by considering correlated molecular changes. Bioinformatics 25:1662–1668
28. **Afonso S, Santamaría I, Guinsburg ME, Gómez AO, Miranda JL, Jofré R, Menárguez J, Cannata-Andía J, Cigudosa JC** 2003 Chromosomal aberrations, the consequence of refractory hyperparathyroidism: its relationship with biochemical parameters. Kidney Int Suppl 85:S32–S38
29. **Cañadillas S, Canalejo A, Santamaría R, Rodríguez ME, Estepa JC, Martín-Malo A, Bravo J, Ramos B, Aguilera-Tejero E, Rodríguez M, Almadén Y** 2005 Calcium-sensing receptor expression and parathyroid hormone secretion in hyperplastic parathyroid glands from humans. J Am Soc Nephrol 16:2190–2197
30. **Ritter CS, Finch JL, Slatopolsky EA, Brown AJ** 2001 Parathyroid hyperplasia in uremic rats precedes down-regulation of the calcium receptor. Kidney Int 60:1737–1744
31. **Ueda K, Arakawa H, Nakamura Y** 2003 Dual-specificity phosphatase 5 (DUSP5) as a direct transcriptional target of tumor suppressor p53. Oncogene 22:5586–5591
32. **Canalejo R, Canalejo A, Martinez-Moreno JM, Rodriguez-Ortiz ME, Estepa JC, Mendoza FJ, Munoz-Castaneda JR, Shalhoub V, Almaden Y, Rodriguez M** 2010 FGF23 fails to inhibit uremic parathyroid glands. J Am Soc Nephrol 21:1125–1135
33. **Hofman-Bang J, Martuseviciene G, Santini MA, Olgaard K, Lewin E** 2010 Increased parathyroid expression of klotho in uremic rats. Kidney Int 78:1119–1127
34. **Stubbs JR, Liu S, Tang W, Zhou J, Wang Y, Yao X, Quarles LD** 2007 Role of hyperphosphatemia and 1,25-dihydroxyvitamin D in vascular calcification and mortality in fibroblastic growth factor 23 null mice. J Am Soc Nephrol 18:2116–2124
35. **Kuro OM** 2011 Phosphate and Klotho. Kidney Int Suppl 121:S20–S23
36. **Patterson KI, Brummer T, O'Brien PM, Daly RJ** 2009 Dual-specificity phosphatases: critical regulators with diverse cellular targets. Biochem J 418:475–489
37. **Groom LA, Sneddon AA, Alessi DR, Dowd S, Keyse SM** 1996 Differential regulation of the MAP, SAP and RK/p38 kinases by Pyst1, a novel cytosolic dual-specificity phosphatase. EMBO J 15:3621–3632
38. **Shin DY, Ishibashi T, Choi TS, Chung E, Chung IY, Aaronson SA, Bottaro DP** 1997 A novel human ERK phosphatase regulates H-ras and v-raf signal transduction. Oncogene 14:2633–2639
39. **Owens DM, Keyse SM** 2007 Differential regulation of MAP kinase signalling by dual-specificity protein phosphatases. Oncogene 26:3203–3213
40. **Chang F, Steelman LS, Lee JT, Shelton JG, Navolanic PM, Blalock WL, Franklin RA, McCubrey JA** 2003 Signal transduction mediated by the Ras/Raf/MEK/ERK pathway from cytokine receptors to transcription factors: potential targeting for therapeutic intervention. Leukemia 17:1263–1293
41. **Canadillas S, Canalejo R, Rodriguez-Ortiz ME, Martinez-Moreno**

JM, Estepa JC, Zafra R, Perez J, Munoz-Castaneda JR, Canalejo A, Rodriguez M, Almaden Y 24 February 2010 The up-regulation of the parathyroid VDR expression by extracellular calcium is mediated by the ERK1/2-MAPK signaling pathway. Am J Physiol Renal Physiol 10.1152/ajprenal.00529.2009

42. **Parisi E, Almadén Y, Ibarz M, Panizo S, Cardús A, Rodriguez M, Fernandez E, Valdivielso JM** 2009 *N*-methyl-D-aspartate receptors are expressed in rat parathyroid gland and regulate PTH secretion. Am J Physiol Renal Physiol 296:F1291–F1296
43. **Bermudez O, Pagès G, Gimond C** 2010 The dual-specificity MAP kinase phosphatases: critical roles in development and cancer. Am J Physiol Cell Physiol 299:C189–C202
44. **Zhang Z, Kobayashi S, Borczuk AC, Leidner RS, Laframboise T, Levine AD, Halmos B** 2010 Dual specificity phosphatase 6 (DUSP6) is an ETS-regulated negative feedback mediator of oncogenic ERK signaling in lung cancer cells. Carcinogenesis 31:577–586
45. **Maillet M, Purcell NH, Sargent MA, York AJ, Bueno OF, Molkentin JD** 2008 DUSP6 (MKP3) null mice show enhanced ERK1/2 phosphorylation at baseline and increased myocyte proliferation in the heart affecting disease susceptibility. J Biol Chem 283:31246–31255
46. **Ekerot M, Stavridis MP, Delavaine L, Mitchell MP, Staples C, Owens DM, Keenan ID, Dickinson RJ, Storey KG, Keyse SM** 2008 Negative-feedback regulation of FGF signalling by DUSP6/MKP-3 is driven by ERK1/2 and mediated by Ets factor binding to a conserved site within the DUSP6/MKP-3 gene promoter. Biochem J 412:287–298
47. **Alvarez-Hernández D, González-Suárez I, Carrillo-López N, Naves-Díaz M, Anguita-Velasco J, Cannata-Andía JB** 2008 Viability and functionality of fresh and cryopreserved human hyperplastic parathyroid tissue tested in vitro. Am J Nephrol 28:76–82
48. **González-Suárez I, Alvarez-Hernández D, Carrillo-López N, Naves-Díaz M, Luis Fernández-Martín J, Cannata-Andía JB** 2005 Aluminum posttranscriptional regulation of parathyroid hormone synthesis: a role for the calcium-sensing receptor. Kidney Int 68:2484–2496